Agricultural and Forest Meteorology 171–172 (2013) 256–269

Contents lists available at SciVerse ScienceDirect

Agricultural and Forest Meteorology

journal homepage: www.elsevier.com/locate/agrformet

Spatial and temporal variability of soil CO_2 efflux in three proximate temperate forest ecosystems

A. Christopher Oishi[a,*], Sari Palmroth[a,b], John R. Butnor[c], Kurt H. Johnsen[d], Ram Oren[a,b,e]

[a] Division of Environmental Science & Policy, Nicholas School of the Environment, Duke University, Durham, NC 27708-0328, USA
[b] Department of Forest Ecology & Management, Swedish University of Agricultural Sciences (SLU), SE-901 83, Umeå, Sweden
[c] Southern Research Station, USDA Forest Service, 81 Carrigan Drive, Aiken Center, University of Vermont, Burlington, VT 05405, USA
[d] Southern Research Station, USDA Forest Service, 3041 Cornwallis Road, Research Triangle Park, NC 27709, USA
[e] Department of Civil & Environmental Engineering, Pratt School of Engineering, Duke University, Durham, NC 27708-0271, USA

ARTICLE INFO

Article history:
Received 26 April 2012
Received in revised form
14 December 2012
Accepted 17 December 2012

Keywords:
Automated soil respiration chambers
Belowground carbon flux
Deciduous
Drought
Evergreen
Litterfall

ABSTRACT

The magnitude of CO_2 flux from soil (F_{soil}) varies with primary productivity and environmental drivers of respiration, soil temperature (T_{soil}) and moisture, all of which vary temporally and spatially. To quantify the sources of F_{soil} variability, we first compared F_{soil} of three proximate forests within 30 km of one another, ranging in age, composition, soil, and environment and, thus, productivity. We collected data with automated soil respiration chambers during a 10-year period in a mid-rotation *Pinus taeda* plantation (PP), for three-years in a mature *P. taeda* stand (OP), and for five-years in a mature, mixed-species hardwood (HW) stand; PP and HW were on clay-loam soil and OP on a sandy soil. Among stands, F_{soil} sensitivity to T_{soil} was lowest in OP and highest in PP, reflected in mean annual F_{soil} (±standard deviation) of 1033 ± 226 (OP), 1206 ± 99 (HW), and 1383 ± 152 (PP) g C m^{-2}; both F_{soil} sensitivity to T_{soil} and annual F_{soil} increased with leaf litterfall. For the second portion of our study, we established an additional three plots at PP for a six-year period to examine within-stand variability. Within PP, sensitivity of F_{soil} to T_{soil} was similar, yet higher leaf area was correlated with a combination of lower soil temperature and belowground carbon flux, resulting in lower F_{soil}. Temporally, diurnal to seasonal F_{soil} followed T_{soil} whereas annual values were driven by soil moisture. Spatially, among the three stands F_{soil} increased with leaf production, whereas within a stand (PP) F_{soil} decreased with increasing leaf production.

1. Introduction

Terrestrial ecosystem respiration is the second largest flux of CO_2 globally, nearly equal to uptake by terrestrial photosynthesis (Raich and Schlesinger, 1992; Schimel et al., 2001). Because the balance between carbon (C) loss and gain greatly influences terrestrial C storage, quantifying the sources of variation of ecosystem respiration is critical for assessing the influence of terrestrial ecosystems on atmospheric CO_2 concentrations.

The largest loss of C from terrestrial ecosystems occurs as CO_2 flux from the soil surface (hereinafter F_{soil}; Ryan and Law, 2005). F_{soil} is comprised of both autotrophic and heterotrophic respiration and is affected by a set of interacting environmental and physiological variables, leading to large variability spatially and temporally (Curiel Yuste et al., 2005; Litton et al., 2007; Martin and Bolstad, 2009). Globally, F_{soil} tends to increase with productivity across biomes (Litton et al., 2007), which implies that both follow mean annual temperature and, to a somewhat lesser extent, precipitation (Bahn et al., 2010; Raich and Schlesinger, 1992; Wang et al., 2010). Although the relationship between annual F_{soil} and soil temperature (T_{soil}) is useful in broad applications, within a biome, mean annual T_{soil} typically does not explain much of the spatial variation of annual F_{soil} within and among forests (Bahn et al., 2010; Janssens et al., 2001; Reichstein et al., 2003; Oishi et al., in preparation). Attempts to account for spatial variability in F_{soil} often focuses on small-scale differences among point measurements within a stand aimed at linking F_{soil} measurements with fine root biomass, proximity to trees, soil C and nutrient content (Martin and Bolstad, 2009; Luan et al., 2012; Søe and Buchmann, 2005). Because F_{soil} integrates many physical and biological processes, several models have been developed to predict surface flux based on production and diffusion through the soil (Daly et al., 2009; Phillips et al., 2011; Suwa et al., 2004). Yet, the amount of information necessary to scale these types of models from a single point to regional or global models is prohibitive. To this end, there is a pressing need to find a pragmatic, middle-ground approach that incorporates simple,

Abbreviations: F_{soil}, soil CO_2 flux; F^*_{soil}, potential soil CO_2 flux under non-limiting soil moisture; LAI, leaf area index; R_{b10}, basal respiration at 10 °C; REW, relative extractable water; T_{air}, air temperature; T_{soil}, soil temperature; T_{10}, T_{soil} at 10 cm; TBCF, total belowground carbon flux.

* Corresponding author. Tel.: +1 919 613 8044; fax: +1 919 684 8741.
E-mail address: acoishi@duke.edu (A.C. Oishi).

0168-1923/$ – see front matter © 2012 Elsevier B.V. All rights reserved.
http://dx.doi.org/10.1016/j.agrformet.2012.12.007

easily measurable variables to explain spatial variability within and among stands.

Underlying the large-scale spatial variability in F_{soil} is the strong exponential increase in F_{soil} with T_{soil} (Davidson and Janssens, 2006; Fang and Moncrieff, 2001). This relationship has been described across wide range of ecosystems and has led to the widespread use of the Q_{10} parameter (the factor by which F_{soil} increases with a change of 10 °C), and R_b (the basal rate of respiration at a reference temperature) in studies of temporal and among-stand variation in soil CO_2 efflux. However, since Q_{10} and R_b integrate all sources of soil CO_2, each with different temperature sensitivities and variability in substrate availability, the "apparent Q_{10}" (i.e. the empirically derived bulk soil Q_{10}) should be calculated and interpreted with caution (Davidson et al., 2006; Trumbore, 2000). The apparent Q_{10} can vary temporally (Curiel Yuste et al., 2005) and among-site/study variation may reflect differences in methodology, such as measurement frequency, sampling depth, and observed temperature range (Davidson et al., 2006; Subke and Bahn, 2010; Wang et al., 2010). Interpretation of the temperature sensitivity of F_{soil} is further complicated by co-variation of environmental drivers and time lags between the biological response to these drivers and the signal in F_{soil}. For example, T_{soil} directly affects enzyme kinetics, but it also co-varies with solar radiation and phenology, and thus belowground photosynthetic inputs (Irvine et al., 2008; Savage et al., 2009). In addition, the seasonal and spatial pattern of T_{soil} likely affects the size of fine root and microorganisms populations (Fenn et al., 2010; Taneva and Gonzalez-Meler, 2011; but see Moyano et al., 2008). Nevertheless, if carefully utilized, the general applicability of a Q_{10} function can still provide a useful, empirical tool for estimating F_{soil} and comparing F_{soil} among sites. Given the widespread measurement of F_{soil}, increasingly done with automated, high-frequency systems, such an approach is particularly valuable.

Soil moisture is the second most important environmental factor affecting F_{soil} as it directly limits microbial activity at low values (Drake et al., 2012; Gaumont-Guay et al., 2006). Drought stress can also limit photosynthesis through stomatal regulation (Oren and Pataki, 2001; Schäfer et al., 2002) which results in decreased fine root production (Pritchard et al., 2008). Under high soil moisture, reduction in air-filled porosity limits soil CO_2 diffusion rates (Maier et al., 2011; Risk et al., 2002; Riveros-Iregui et al., 2007; Suwa et al., 2004). Previous findings in warm temperate climates demonstrate that under non-limiting soil moisture conditions, F_{soil} is driven by variation of soil temperature diurnally and seasonally, while inter-annual variation of F_{soil} is controlled by variation of soil moisture (Maier et al., 2004; Palmroth et al., 2005; Oishi et al., in preparation).

Given the above, within a restricted geographic region where mean annual temperature and precipitation are similar, can among-stand characteristics explain variability in F_{soil}? One characteristic that is well correlated with F_{soil} is leaf production (Bahn et al., 2010; Bond-Lamberty and Thomson, 2010; Chen et al., 2010; Davidson et al., 2002; Nadelhoffer and Raich, 1992; Palmroth et al., 2005). Leaf production, quantified as either leaf litterfall or leaf area index (LAI), is a reasonable proxy for overall productivity and provides several compelling, yet not necessarily straightforward links to F_{soil}. First, LAI can directly impact the local environment. For example, higher LAI reduces radiation and precipitation reaching the forest floor and increases transpiration, resulting in cooler and dryer soil conditions (Ngao et al., 2012; Palmroth et al., 2005; Phillips et al., 2010). Second, leaf litterfall supplies much of the substrate for the heterotrophic component of F_{soil}. Third, because the autotrophic component of F_{soil} typically exceeds the heterotrophic component, F_{soil} must also depend upon substrate supplied through primary productivity and thus the partitioning of recently assimilated C belowground (Johnsen et al., 2007; Högberg et al., 2008; Mencuccini and Hölttä, 2010).

Autotrophic respiration of all biomass components generally increases with gross primary productivity (GPP; DeLucia et al., 2007; Litton et al., 2007). Leaf area index increases with resource availability (e.g. site fertility and water-supply) and is accompanied with increased GPP up to the point at which light absorption no longer increases with LAI. Palmroth et al. (2006) showed that across young forests of different species, F_{soil} seemed to increase with LAI when LAI was very low, essentially reflecting increasing soil volume occupation by roots. However, among stands with moderate to high LAI, when GPP no longer increases with LAI, higher wood production aboveground is at the expense of C allocated to support fast turning soil pools such as F_{soil} (McCarthy et al., 2006; Palmroth et al., 2006; Oishi et al., in preparation).

In our previous studies we found that a mid-rotation loblolly pine plantation (PP) and a mature mixed-species deciduous hardwood stand (HW), both on clay-loam soil and similar maximum LAI, showed similar sensitivities of F_{soil} to T_{soil} and soil moisture. However, different LAI dynamics and forest floor thickness affected both these variables, resulting in different annual F_{soil}. Roughly, ~1 °C higher mean annual T_{soil} caused ~10% higher F_{soil} (Palmroth et al., 2005). In contrast, within a single PP plot, ~1 °C higher T_{soil} (in years with low LAI) resulted in ~60% higher F_{soil}. This indicates that variation of C flux to belowground pools, possibly linked to variation of LAI, can have a greater effect on interannual variability of F_{soil} than environmental variables (Butnor et al., 2003; Palmroth et al., 2006).

In this study, we test three hypotheses on the sources of spatial and temporal variability among and within forest stands experiencing similar climatic forcing and test whether the variability can be linked to productivity indicators. Our first hypothesis (H1) is that in all stands, inter-annual variability T_{soil} is small and thus, inter-annual variability of F_{soil} is driven by precipitation and thus soil water availability. Second, we hypothesize (H2) that, among forest stands, increasing primary productivity, as reflected in leaf production, results in greater temperature-sensitivity of soil CO_2 efflux and higher annual F_{soil}. And third, we hypothesize that within a stand, increasing leaf production corresponds with lower annual F_{soil} as a result of (H3.a) reduced belowground carbon supply, which leads to lower temperature-sensitivity of F_{soil}, or (H3.b) decreased radiation reaching the forest floor, which leads to lower T_{soil}.

We expand on previous work by extending the measurement period to ten years at PP and five years at HW and including new data spanning six years from three adjacent plots within the PP stand and a mature loblolly pine stand on a low-fertility, sandy soil (old pine; OP). All three stands were within 30 km in the Piedmont region of North Carolina, USA and experienced similar environmental conditions but, due to differences in site fertility and stand composition, ranged in substantially in productivity.

2. Materials and methods

2.1. Study sites

The study was conducted in three stands within Duke Forest in central North Carolina, USA (see Table 1 for site and stand characteristics). An 18 year-old maturing loblolly pine plantation (PP) and 80–100 year-old mixed-species deciduous hardwood stand (HW) are adjacent stands in the Blackwood Division, within 1 km of one another. Soil at both of these sites have moderate water-holding capacity in the upper layer, but low permeability in the lower level, so it does not readily release water to plants (Soil Survey of Orange County, 1977). The PP plots are part of the Duke Free Air CO_2 Enrichment (FACE) site, but measurements for this study were taken in

Table 1
Site characteristics for three Duke Forest stands: pine plantation (PP), hardwood (HW), and old pine (OP).

	PP	HW	OP
Coordinates (Lat, Lon)	35°58′N, 79°08′W	35°58′N, 79°08′W	36°12′N, 79°17′W
Elevation (m)	160	160	212
Stand characteristics			
Stand age (years old in 2001)	18	~80–100	~35
Stem density (trees ha^{-1})	3200	930	300
Basal area ($cm^2\ m^{-2}$)	42	22	28.5
Height (m)	20	35	25
Peak LAI ($m^3\ m^{-3}$)	5.8	7.0	2.0
LAI by species (%)			
Pinus taeda	54	0	78
Liriodendron tulipifera	Not available[a]	12	Not available[a]
Liquidambar styraciflua	Not available[a]	10	Not available[a]
Carya spp.	Not available[a]	30	Not available[a]
Quercus spp.	Not available[a]	18	Not available[a]
Other deciduous	45	29	22
Soil characteristics			
Soil type	Enon silt loam Acidic clay-loam	Iredell gravelly loam	Durham sandy loam
Porosity ($m^3\ m^{-3}$)	0.540	0.540	0.500
Field capacity ($m^3\ m^{-3}$)	0.350	0.350	0.200
Hygroscopic point ($m^3\ m^{-3}$)	0.125	0.125	0.050
Site slope (%)	<5	<3	<5
Rock content (%)	12.5	Not measured	Not measured
Coarse fragment (%)	13.5	14.3	Not measured
Rooting depth (m)	0.30	0.30	2.00

[a] LAI from deciduous trees was not separated by individual species at PP or OP.

four ambient CO_2 in plots in sectors without nitrogen amendments. Sampling at HW was at the base of the Duke Hardwood Ameriflux tower.

The third stand was a 35 year-old mature loblolly pine stand (old pine; OP), located in the Dailey Division of Duke forest, approximately 30 km northwest of the other two stands. This site was thinned in 1993 and 1998, leaving a partially open canopy with a small hardwood understory. The OP stand had deeper soil that drained rapidly, as opposed to PP and HW, which had a low-permeability clay layer at 0.35 m (Table 1; Soil Survey of Alamance County, 1960; Oren et al., 1998).

2.2. Instrumentation

Air temperature (T_{air}) was measured with sensors installed at 2/3 canopy height (HMP35C, Campbell Scientific, Logan, UT), and incoming precipitation was measured at each site with above-canopy tipping bucket installed at the top of a walkup tower (TE525M, Texas Electronics, Dallas, TX).

Soil temperature was measured with permanently installed thermistors (334-NTC102-RC, Xicon Passive Components, Mansfield, TX) buried at 10 cm (T_{10}). Soil temperature was averaged among five thermistors at HW and six at OP. Spatial variability in T_{10} among the sensors was small; the coefficient of variation (CV) for the year was less than 9.5% (6.3% and 9.4% for HW and OP, respectively). The greatest variability occurred during the winter when temperatures and fluxes were low, so growing season CVs were less than 5.0% (2.7% and 4.9%, respectively). Only one of the PP plots had more than one thermistor installed at 10 cm, but variability of daily T_{10} in this plot was also low (mean annual and growing season CVs were 4.2% and 2.7% respectively; $n = 4$). Soil moisture (θ) was measured at each PP plot as volumetric water content with two time domain reflectometry sensors (CS-615, Campbell Scientific, Logan, UT) installed vertically, integrating over 0–30 cm depth. At HW and OP θ was measured with vertically oriented frequency domain sensors (ThetaProbe ML2x, Delta-T Devices, Cambridge, UK). We deployed six sensors at HW and four at OP, half at 0–5 cm and half at 20–25 cm, and a stand-level average θ was generated averaging data from all sensors at both depths. Data were filtered to eliminate unrealistic spikes immediately following rain events (see Appendix A).

To normalize soil moisture amongst stands and increase the generality of our results, soil moisture is expressed in this study as relative extractable water ($REW = (\theta - \theta_m)/(\theta_{FC} - \theta_m)$; Granier, 1987), where θ is the volumetric water content, θ_m is the hygroscopic point where soil water is no longer available for plants, and θ_{FC} is θ at field capacity. At both PP and HW, θ_m was 0.125 $m^3\ m^{-3}$ and θ_{FC} was 0.35 $m^3\ m^{-3}$, respectively. At OP, θ_m was set to the recorded value where soil moisture hit the stable, minimum point in the drought of 2005 ($\theta = 0.05\ m^3\ m^{-3}$) and θ_{FC} was set to the average value reached during non-growing season months at least two days after large precipitation events ($\theta = 0.20\ m^3\ m^{-3}$).

2.3. Leaf litterfall and leaf area index

Leaf litter was collected periodically throughout the study with an array of baskets at each site and used to estimate litter mass and LAI. Data from PP and HW have been presented in McCarthy et al. (2007) and Oishi et al. (2008), respectively.

At OP, litter was collected in ten 0.5 m^2 baskets, oven dried, sorted into pine and hardwood components, and weighed for total mass. Leaf area index (LAI) was estimated from total litter mass and specific leaf area, measured using a light table or digital scanner. Time trends of LAI were measured with an optical plant canopy analyzer (LAI-2000, Li-Cor, Lincoln, NE). Since LAI at OP was lower than the point of optical saturation (McCarthy et al., 2007), data from the LAI-2000 at OP was not rescaled to match litter-based LAI estimates.

2.4. Soil CO_2 efflux

F_{soil} was measured using the Automated Carbon Efflux System (ACES, USDA Forest Service, US Patent 6,692,970). The system has been described in previous studies (Butnor et al., 2003;

Table 2
Number of operational days for each ACES. Blank cells indicate that no system was installed during that year. Zero values indicate that no useable data was recoverable from that year.

	2001	2002	2003	2004	2005	2006	2007	2008	2009	2010
PP1					96	270	253	237	123	88
PP5						176	161	204	94	67
PP6					99	174	0	164	0	43
PP8	149	268	181	202	145	199	234	0	0	142
HW	172	290	246	295	43					
OP			179	178	45					

Palmroth et al., 2005); briefly, it is an IRGA-based open system that sequentially samples 15 chambers plus one null chamber (491 cm^2 footprint, 10 cm height). Each chamber is sampled for a 10-min cycle and the final record is accepted if air flow rates and CO_2 concentrations are stable and within a specified range; thus there can be a maximum of 9 measurements for each chamber throughout each day.

Terms relating to the spatial aggregation of samples are described as follows: *location* refers to a measurement taken at a specific soil efflux chamber in a specific position, *plot* refers to an array of chambers connected to a single ACES (~25 m diameter range), and *stand* refers to a forested area with a similar age, species composition, and soil characteristics (~1 km diameter). The HW and OP stands each consisted of one plot established in 2001 and 2003, respectively, and ran through early 2005 (Table 2). Of the four PP plots, PP8 (the number referring the FACE plot number) includes data from 2001 to 2010. Additional ACES were added to PP1 and PP6 in early 2005 and PP5 starting in 2006 (this setup included redeployed ACES from HW and OP). For each of the ACES, four of the chambers were connected to tree stems and data collected are not used in this study. In PP plots, five of the remaining chambers were located in the N-fertilized sectors of the FACE plots. Therefore, PP consists of data from six chambers while HW and OP consist of data from 11 chambers.

Each chamber was alternated between one of two fixed *locations* in the plot and ran in a given position for 3–4 day periods. Chamber movement is intended to minimize chamber effects on the amount of litter and moisture arriving at the monitored surface, and to increase the spatial sampling. Chamber locations were changed several times during the study period, initially to minimize disturbance to a sampling area and later to examine variability with proximity to trees. The chamber bases have a sharp, metal edge that extend beneath the soil surface approximately 1 cm, but do not use a permanently installed collar. Upon initial location establishment, each chamber's metal edge is used to cut into the soil surface. This shallow circular trench is maintained by the presence of the sampling chamber or an open-top, circular plastic placeholder ring, thereby preventing the chamber location switches from severing new fine root growth. Litter excluded during measurement cycles was replenished (Appendix B).

ACES are designed to run continuously; however, several factors reduced the amount of usable data. First, individual measurements were filtered to exclude sampling periods where either air flow or CO_2 concentrations were out of range. Second, systems were offline periodically for general maintenance and recalibration. Third, over the long duration of the study, systems were offline for repair more frequently. Therefore, the measurements were not continuous throughout the study period. In the case of PP6 and PP8, few short segments between repairs beginning in 2009 and 2008, respectively, forced us to exclude these data (Table 2). Nevertheless, measurements did encompass much of the environmental variability that occurred over the past decade, including several droughts and wet growing seasons (Table 3).

To analyze the sensitivity of F_{soil} to environmental variables and to fill gaps in data coverage, we utilized the model for F_{soil} as a function of T_{soil} and REW previously described in Palmroth et al. (2005):

$$F_{soil} = F^*_{soil} \times f(\mathrm{REW}) \quad (1)$$

where F_{soil} is mean daily soil CO_2 flux for a specific location for days when at least 5 measurements were taken ($\mu mol\ CO_2\ m^{-2}\ s^{-1}$), F^*_{soil} is potential F_{soil} for a given T_{10} under non-limiting REW, and f(REW) is a unitless function describing the limitations to F_{soil} imposed by REW. Our approach to fit parameters proceeded as follows. We first estimated F^*_{soil} by fitting measured F_{soil} from each chamber location as a function of T_{10} under non-limiting soil moisture conditions. These conditions were defined as REW > 0.33 in PP and HW (equivalent to $\theta > 0.20\ m^3\ m^{-3}$ in Palmroth et al., 2005) and as REW > 0.45 at OP, the point below which F_{soil} was on average 90% of the values in wetter conditions. The form used is

$$F^*_{soil} = R_{b10}\exp(b(T_{10} - 10)) \quad (2)$$

where T_{10} is daily mean T_{soil} (°C) at 10 cm for the corresponding plot, R_{b10} is estimated "basal" respiration at 10 °C ($\mu mol\ CO_2\ m^{-2}\ s^{-1}$), and b is the temperature sensitivity parameter ($\exp(b \times 10) = Q_{10}$). The values of F_{soil} were Log_e transformed so the data could be fit as a linear function using the ACOTOOL function in Matlab (Version 6.0.1.450, Release 12.1, MathWorks Inc.), with year as a categorical variable. Linear regressions were not possible for all locations in all years due to limitations in data for reasons described previously as well as uneven representation of T_{10} ranges. For example, during the drought year of 2005, there were very few days with temperature above the annual mean and non-limiting soil moisture. Least squares fitting of these data led to some unreasonable Q_{10} values (e.g. <0). Therefore, we constrained each location's regressions by assuming a constant Q_{10} parameter across years, but allowing for varying R_{b10}.

Limitations to F_{soil} imposed by REW, f(REW), were accounted by fitting the proportionate reduction from F^*_{soil} under non-limiting REW using Matlab's least-squares, nonlinear NLINFIT function for each chamber location:

$$f(\mathrm{REW}) = 1 - \exp(-c \times \mathrm{REW} + d) \quad (3)$$

where c and d are coefficients describing the sensitivity of F_{soil} to low REW. The combination of few low-REW days during some years and gaps in observations in some plots in other years did not provide us with enough data to fit f(REW) independently for each year. However, two of the driest years, 2005 and 2007, we were able to fit f(REW) for two PP plots to test for interannual differences in the c and d coefficients. Neither c nor d was different between the two years ($P > 0.20$; t-test). Thus, data were pooled across years to allow estimation of f(REW) parameters over sufficiently wide range of soil moisture and so represented the entire study period.

In both analyses, parameters from each chamber location and from each of the years with enough data were within the 95% confidence interval of parameters generated from the fit of the pooled data of all years 78% of the time. For the four years before ACES were

Table 3
Mean annual and growing season (DOY 100–285) soil temperature at 10 cm (T_{10}; °C) and soil relative extractable water (REW).

	2001	2002	2003	2004	2005	2006	2007	2008	2009	2010
Mean annual T_{10}										
PP1		14.95	14.28	14.74	14.45	14.56	14.85	14.62	14.41	14.17
PP5		14.39	13.80	14.21	13.97	14.07	14.28	13.99	13.94	13.81
PP6		15.19	14.53	14.97	14.86	15.20	16.12	14.91	14.95	14.87
PP8	14.38	14.18	13.72	13.93	13.74	13.75	14.00	13.70	13.59	13.38
HW	14.94	15.58	15.17	15.40	15.22					
OP			15.43	15.51	14.60					
Mean growing season T_{10}										
PP1		19.53	18.98	19.43	19.00	18.66	18.76	18.65	18.73	19.40
PP5		18.46	17.97	18.32	17.97	17.76	17.90	17.77	17.73	18.40
PP6		19.68	19.14	19.69	19.46	19.08	19.72	18.96	19.42	19.99
PP8	18.62	18.86	18.27	18.59	18.19	17.77	17.85	17.64	17.71	18.24
HW	19.92	20.69	20.08	20.46	20.12					
OP			20.54	20.19	19.06					
Mean annual REW										
PP1	0.55	0.60	0.74	0.74	0.51	0.61	0.44	0.70	0.63	0.50
PP5	0.55	0.61	0.74	0.74	0.51	0.60	0.43	0.69	0.63	0.51
PP6	0.51	0.59	0.73	0.74	0.54	0.61	0.43	0.65	0.59	0.44
PP8	0.54	0.59	0.74	0.73	0.52	0.62	0.45	0.66	0.61	0.47
HW	0.64	0.68	0.90	0.84	0.70					
OP			0.80	0.70	0.58					
Mean growing season REW										
PP1	0.48	0.26	0.64	0.59	0.26	0.43	0.24	0.59	0.38	0.31
PP5	0.46	0.27	0.65	0.60	0.27	0.42	0.22	0.60	0.38	0.32
PP6	0.43	0.24	0.67	0.59	0.32	0.42	0.24	0.57	0.34	0.27
PP8	0.46	0.24	0.68	0.57	0.27	0.44	0.26	0.60	0.37	0.31
HW	0.57	0.39	0.83	0.74	0.55					
OP			0.77	0.62	0.40					

installed in PP1, PP5, and PP6, we estimated F_{soil} using measured T_{10} and REW and mean, plot-level parameters.

Matlab was also used to process raw data and for linear regressions and statistical tests. SigmaPlot (v8.0.2, SPSS Inc.) was used for additional curve fitting.

3. Results

We collected 283,572 data points across 6 plots between 2001 and 2010, accounting for 31 "plot-years" (Table 2), allowing us to analyze variability in soil CO_2 efflux (F_{soil}) across temporal and spatial scales. We first analyzed the temperature- and soil moisture-sensitivities among different stands and among plots within the maturing pine plantation (PP). We then estimated annual F_{soil} to examine to what extent differences in environmental drivers are leading to variability among stands and plots. Finally, we examined whether leaf productivity explained variability among stands and plots.

3.1. Soil temperature and moisture sensitivity of daily F_{soil}

Soil moisture (i.e. relative extractable water; REW) and temperature (T_{10}) showed strong seasonal variability (Fig. 1). During winter months REW stayed near field capacity (REW ≈ 1.0) and the soil dried progressively during much of growing season (Table 3).

Between 66 and 82% of variability in daily soil CO_2 efflux under non-limiting REW (F^*_{soil}) was explained by T_{10} across all plots (Eq. (2); Table 4; Appendix C). At PP, mean R_{b10} values were similar among plots ($P = 0.39$), but Q_{10} differed ($P < 0.0001$, although some pairs of plots were similar; Table 4). An inverse relationship was found between Q_{10} and R_{b10} among plots within PP ($P = 0.09$; $r^2 = 0.82$), such that the overall temperature sensitivity of F^*_{soil} was similar among plots over the majority of the range of T_{10} (Fig. 2a). In other words, no plot had consistently higher or lower F^*_{soil} over the entire T_{10} range. However, Q_{10} and, less significantly, R_{b10} differed among stands ($P < 0.003$; but $P = 0.16$ for R_{b10} differences between HW and OP; Table 4). Overall, PP exhibited the highest F^*_{soil} across the range of temperatures, followed by HW and then OP (Fig. 2b).

During the growing season, low REW led to reductions in F_{soil} in all plots and stands. The soil moisture reduction function (f(REW), Eq. (3)) explained approximately 50% of the variability remaining in daily F_{soil} after accounting for T_{10} (Fig. 2c and Table 4). Parameter estimates for REW reduction functions were different among PP plots ($P < 0.003$, Table 4), reflecting greater reduction in F_{soil} with REW in PP8 than PP6, but PP1 and PP5 were not consistently higher or lower than another plot across the range of REW. Among stands, parameters at HW and OP were similar ($P > 0.13$), but the d parameter at PP was higher than the other two stands ($P = 0.04$). The values of c and d parameters were positively correlated ($r^2 = 0.39$, $P < 0.001$). An increase in the c parameter causes f(REW) to begin declining at a lower REW while an increase in the d parameter reduces f(REW). Thus, the differences among both the c and d parameters compensated for one another among stands,

Table 4
Parameters for estimating soil CO_2 flux under non-liming soil moisture conditions (F^*_{soil}, see Eqs. (1) and (2)) and limitations as a function of relative extractable water (REW, see Eqs. (1) and (3)). SD in parentheses and superscript letters for parameters represent significant similarities among PP plots ($P > 0.05$).

	F^*_{soil}			f(REW)		
	Mean R_{b10}	Q_{10}	r^2	c	d	r^2
PP1	2.16 (0.60)^{ABCD}	3.25 (0.27)^{ACD}	0.80 (0.04)	5.35 (0.98)^{AB}	−0.42 (0.18)^{ABC}	0.52 (0.02)
PP5	1.91 (0.42)^{ABCD}	3.83 (0.36)^{BC}	0.82 (0.07)	4.41 (1.45)^{AB}	−0.71 (0.25)^{ABC}	0.50 (0.02)
PP6	2.07 (0.83)^{ABCD}	3.58 (0.52)^{ABC}	0.71 (0.11)	9.52 (3.03)^{CD}	−0.31 (0.30)^{ABCD}	0.50 (0.04)
PP8	2.15 (0.35)^{ABCD}	3.00 (0.42)^{AD}	0.77 (0.12)	7.89 (2.92)^{CD}	−0.01 (0.56)^{CD}	0.52 (0.03)
HW	1.59 (0.32)	2.97 (0.39)	0.71 (0.11)	7.01 (5.81)	−0.62 (1.11)	0.48 (0.02)
OP	1.46 (0.51)	2.71 (0.31)	0.66 (0.12)	6.26 (3.30)	−0.48 (0.58)	0.46 (0.02)

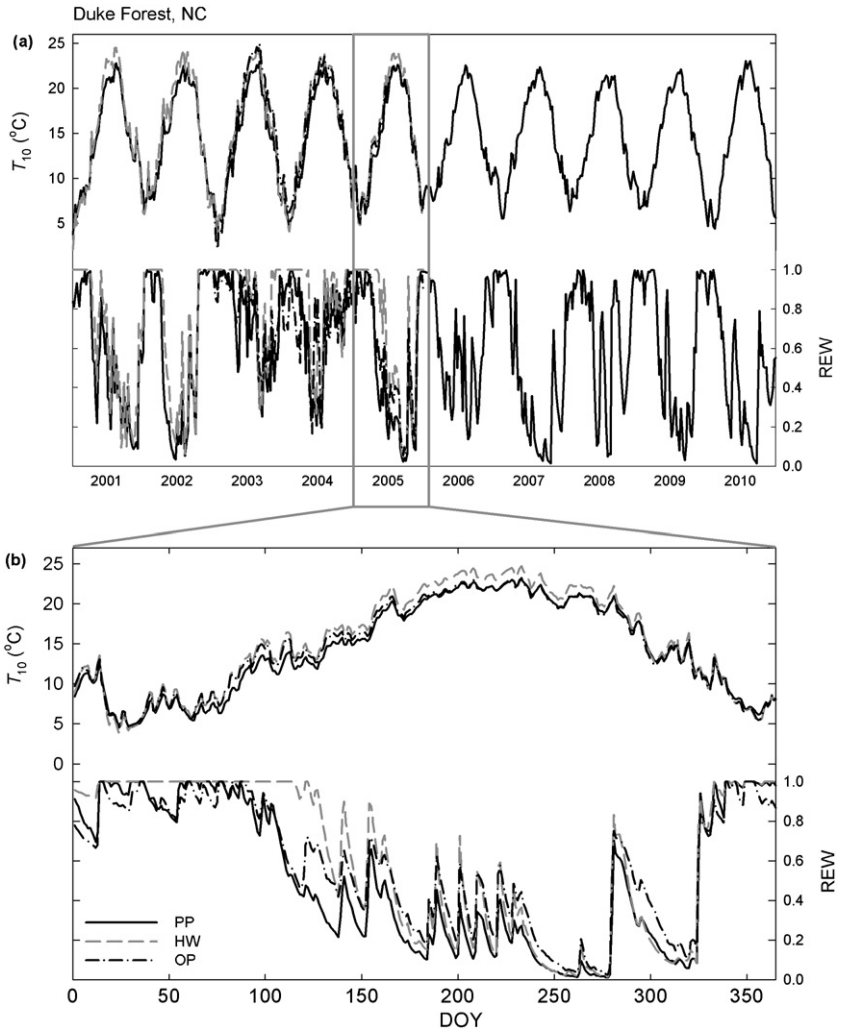

Fig. 1. Soil temperature at 10 cm (T_{10}) and soil moisture as relative extractable water (REW) averaged weekly for the study period (a) and averaged daily for a sample drought year (b).

resulting in similar sensitivities of F_{soil} to soil moisture: f(REW) from each stand was within one standard deviation of the other two stands across the range of REW (Fig. 2d). Reductions in F_{soil} due to soil moisture limitation at HW was within 2% of PP for values of REW as low as 0.15, at which point PP declined more sharply. Reductions in F_{soil} at OP were within 5% of PP for REW as low as 0.25.

Under soil moisture-limited conditions (REW $\leq$ 0.33), F_{soil} showed a rapid response to precipitation during the growing season in all stands, increasing by an average of 20% (SD = 34%, $P < 0.001$; data not shown). The precipitation-induced increases of F_{soil} tended to bring drought-period fluxes close to, but rarely above the expected non-drought values. Small precipitation events (<5 mm) were not detected by soil moisture sensors and did not affect F_{soil} ($P = 0.90$); of precipitation $\geq$5 mm, the amount did not affect the response ($P > 0.37$). We did not observe a reduction in F_{soil} at soil moisture higher than field capacity ($P = 0.06$).

3.2. Sources of variation of annual F_{soil} among plots and years

Annual F_{soil} varied among plots and years (Fig. 3a and b). Of the PP plots, PP8 generally had the lowest F_{soil} while PP1 and PP6 produced the highest fluxes. At the stand level, PP had the highest F_{soil}, followed by HW, then OP. Interannual variability of potential F_{soil} (i.e. F^*_{soil}) was generally low, with plot-level standard deviations ranging from 64 to 193 g C m^{-2} y^{-1} (average CV = 7.7%) somewhat lower than the range of actual F_{soil}, which accounts for limitations by REW (107–218 g C m^{-2} y^{-1}; average CV = 12.2%).

Over the study period, mean annual T_{10} showed small variability within each site and plot (Fig. 1a and Table 3), with site- or plot-level interannual standard deviations <0.5 °C or less than 1 °C differences between highest and lowest annual T_{10} (with the exception of 1.5 °C at PP6). Much of the variability in mean annual T_{10} originated from the non-growing season (mean 8.3 °C, SD = 0.8 °C), a period of little influence on annual F_{soil}. During the growing season, the average T_{10} (=19.2 °C) was associated with small variability (SD = 0.4 °C). Interannual variability in growing season T_{10} was not correlated with LAI ($P > 0.42$) with the exception of PP8 ($P = 0.026$), the plot with the highest leaf productivity. Thus, *interannual* variability in F_{soil} was dependent on other factors.

Unlike T_{10}, REW showed large interannual variability, depending on the magnitude and frequency of precipitation events during the growing season (Fig. 1a and Table 3). Severe drought conditions occurred in 2002, 2007, and 2010 and a moderate drought in 2005; our measurements captured two of these droughts at HW (2002 and 2005) and one at OP (2005). Both annual and growing season REW was highest at HW, followed by OP and then PP (Fig. 1b and Table 3). Comparing the three stands, PP showed the greatest reductions of F_{soil} from F^*_{soil} (i.e. annual f(REW) or F_{soil}/F^*_{soil}, Fig. 3c). The lowest annual f(REW) occurred during the four drought

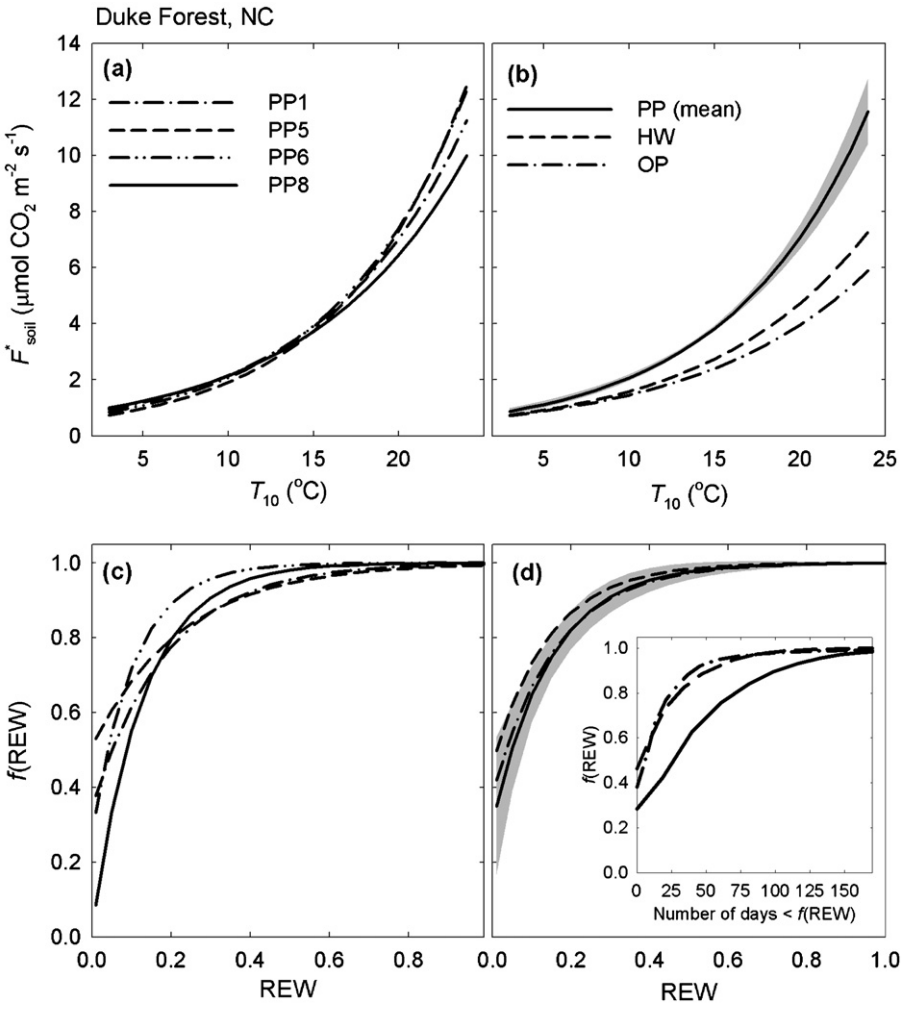

Fig. 2. Response of potential soil CO_2 flux under non-limiting soil moisture (F^*_{soil}) to soil temperature at 10 cm (T_{10}) across all years (a and b) and relative reduction of soil CO_2 efflux (F_{soil}) from F^*_{soil} due to a decrease in relative extractable water (f(REW)) as a function of relative extractable water (REW) (c and d). Data from PP plots are presented in (a and c) and for all stands in (b and d), including the mean and SD (shaded gray) for the four PP plots. The cumulative effect of f(REW) based on recorded REW values in the drought year of 2005 in presented in Fig. 4d inset.

years. Under the extreme drought conditions of 2007, F_{soil} at PP was 73% of potential. Across the study period and stands, annual f(REW) was similarly driven by mean growing season REW (Fig. 4a; $P < 0.0001$). The non-linearity in the response of *daily* f(REW) to REW (Fig. 2c) is also apparent between the *annual* average values (Fig. 4a). However, because F_{soil} was gapfilled using REW data, we also compared growing season f(REW) with an independently measured growing season index of water availability (WAI) defined as precipitation minus pan evaporation (from a nearby NOAA weather station; www.ncdc.noaa.gov; Fig. 4b). At PP, where the greatest range in WAI was available, the relationship between WAI and REW was non-linear (inset in Fig. 4b; $P = 0.035$ for quadratic fit; F-test comparison of polynomial fit over linear fit, $P = 0.076$). Across the range of WAI, REW was lower at PP than at HW and OP (Fig. 4b inset; $P = 0.032$; however, HW and OP were similar, $P = 0.68$). Thus, the non-linearity between REW and f(REW) and between WAI and REW resulted in a linear increase in f(REW) with WAI (Fig. 4b; linear regressions for HW and OP were similar, $P = 0.85$). Compared to the other stands, F_{soil}/F^*_{soil} was lower at PP across the common range in WAI ($P = 0.01$ for difference in intercept).

Annual R_{b10} was unrelated to either REW or WAI ($P > 0.37$). Thus, the frequency of limiting REW conditions largely determines reductions in F_{soil} and was the primary source of the interannual variability in F_{soil}. For example, F_{soil} was reduced to less than 60% of non-limited conditions 37 of days during 2005 at PP, compared to about 10 days at HW and OP; reductions to at least 80% occurred 70, 30, and 25 days in the three stands, respectively (Fig. 2d inset).

3.3. Relationships between mean inter-annual fluxes, stand characteristics, and environmental variables

The variation of mean annual F^*_{soil} among the three stands was best explained by leaf litterfall ($P = 0.004$; Fig. 5a). LAI was not well correlated with litterfall across stands ($P = 0.43$), and produced a weaker relationship with F^*_{soil} ($P = 0.12$, data not shown). Assuming that soil C was in near equilibrium over the study period, and subtracting leaf litterfall C from F^*_{soil} gives a rough estimate of total belowground carbon flux (TBCF; Giardina and Ryan, 2002). The estimates of TBCF also increased with leaf litterfall across stands ($P = 0.005$; Fig. 5a). Across PP plots, F^*_{soil} and TBCF showed weak inverse correlations with leaf litterfall ($P = 0.19$ and 0.13, respectively; Fig. 5a). However, leaf litterfall did not explain the variation in F_{soil} among years at any of the sites ($P > 0.41$; data not shown). Nor was litterfall or LAI related to the parameters of f(REW) across stands ($P > 0.61$) or within PP ($P > 0.70$). The inter-annual variation of F_{soil} across all stands and PP plots (represented as the annual deviation from the interannual mean; Fig. 5b) was explained to a

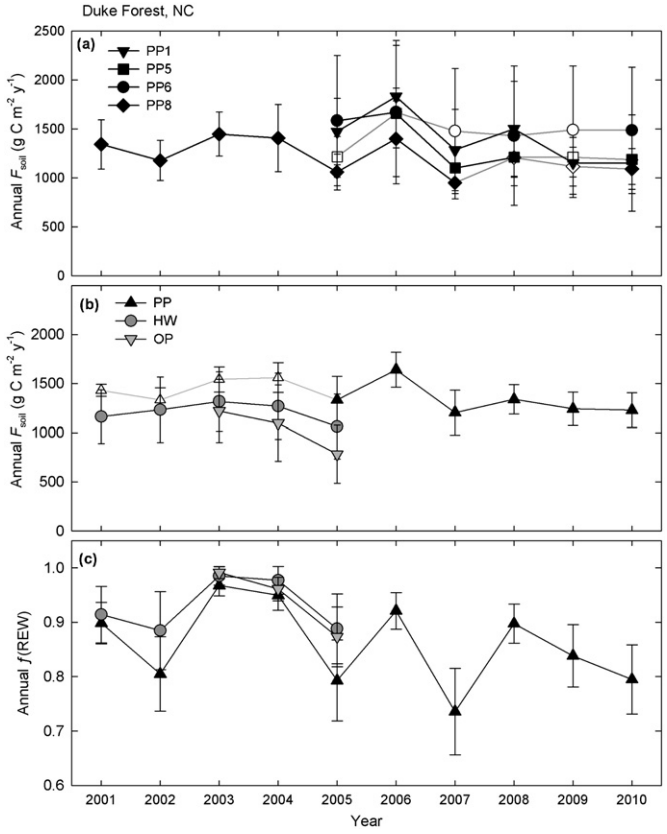

Fig. 3. Estimated annual soil CO_2 flux (F_{soil}) at (a) individual PP plots, and (b) the three forest stands. (c) Deviation of F_{soil} from potential F_{soil} (f(REW), estimated F_{soil} from exponential functions under non-limiting soil moisture; Eq. (2). Error bars represent 1 SD. Solid/shaded symbols are estimated annual sums from measurements taken throughout the year and gapfilled with parameters estimated from that year's data. Open symbols represent annual sums from years when too few measurements were available to estimate parameters and average parameters from other years were used for gapfilling (see Table 4).

large extent by the inter-annual variation of WAI ($P = 0.004$). The relationship was similar among the stands ($P > 0.42$).

Although mean *non-growing* season T_{10} was similar among PP plots and among all stands ($P > 0.07$), mean *growing* season T_{10} at PP was 1.8 °C lower than in HW (Fig. 1a and Table 3). This indicates that among-stand differences in LAI alone could not explain variation in T_{10} ($r^2 = 0.04$; $P = 0.87$). However, Q_{10} (and R_{b10}) increased with leaf litterfall ($P = 0.06$ and 0.14, respectively; Fig. 6a and b), and the resulting among-stand differences in the temperature response of F_{soil} (Fig. 1b) more than compensated for differences in T_{10} (Table 3). In contrast, the temperature response of F_{soil} was similar in all PP plots and unrelated to LAI or leaf litterfall ($P > 0.86$; data not shown). Similarly, neither LAI nor leaf litterfall were related to the individual temperature-sensitivity parameters (Q_{10} or R_{b10}; $P > 0.51$, data not shown), or the combined effect of these parameters based on estimated F^*_{soil} at the mode annual T_{10} (21 °C; $P > 0.18$). Among PP plots, leaf litterfall was well correlated with mean annual LAI (Fig. 7a; $P = 0.06$), and mean growing-season T_{10} decreased with increasing LAI (ranging 1.2 °C among plots; Fig. 7b; $P = 0.25$). Thus, mean annual F^*_{soil} increased with T_{10} (Fig. 7c; $P = 0.063$), yet an inverse relationship with LAI was even stronger (Fig. 7d; $P = 0.069$). Taken together, the differences in T_{10} contributed 55–85% to the difference of F^*_{soil} among plots with the remaining differences explained by between-plot differences in Q_{10} (Table 4).

4. Discussion

Two broad classes of factors can contribute to spatial and inter-annual variation of F_{soil}: (1) the temperature- and moisture-sensitivity of the flux, reflecting differences in attributes such as litter quality and C availability, and (2) variation in temperature and moisture, reflecting incoming radiation and water availability, which are related to topography and soil characteristics but also to forest attributes such as LAI. Our study shows that that leaf litterfall works as an index of stand-level F_{soil} only over a wide range of productivity (e.g. among stands). Within a narrower spatial scope, such as within a forest stand that encompasses a smaller range in productivity, LAI is inversely related to physical (soil temperature and moisture) and physiological (belowground C supply) factors driving F_{soil}. At this smaller scale, LAI can therefore provide some insight into the relationship between above- and belowground C allocation.

Our results support the first hypothesis (H1); in all stands, inter-annual variability T_{soil} was small and thus, interannual variability of F_{soil} was driven by precipitation and thus soil water availability. The seasonal dynamics of F_{soil} corresponded to those of T_{10} at all chamber locations and, thus, plots and stands. When soil moisture was non-limiting, increased T_{10} resulted in an exponential rise of

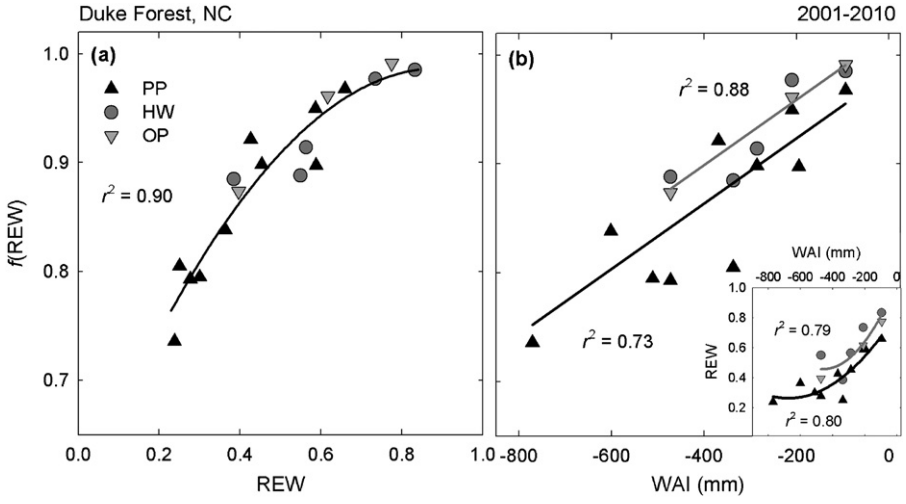

Fig. 4. Proportionate departure of annual soil CO_2 flux (F_{soil}) from potential F_{soil} due to relative extractable water (REW) reduction function (f(REW)) and (a) mean growing season REW and (b) growing season water availability index (WAI, the difference between growing season precipitation and pan evaporation). Inset in (b) is the relationship between WAI and REW.

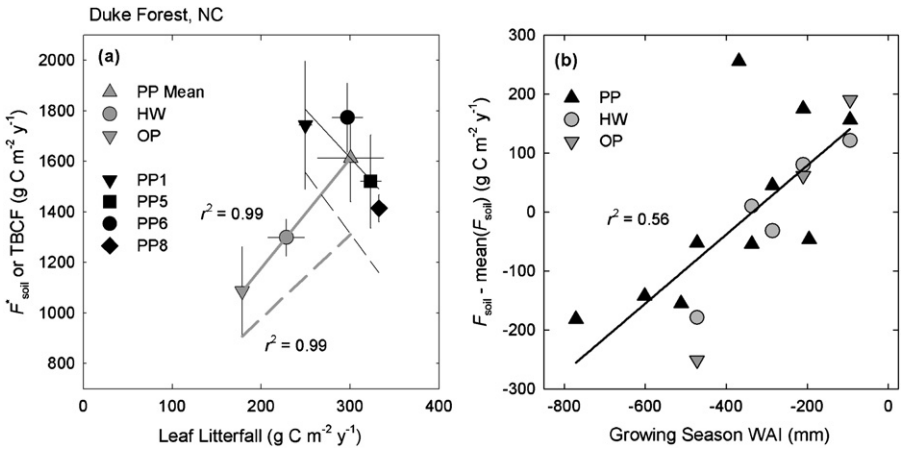

Fig. 5. (a) Annual potential soil CO_2 flux under non-limiting soil moisture conditions (F^*_{soil}, symbols and solid lines) or total belowground carbon flux (TBCF = F^*_{soil} minus leaf litterfall) as a function of annual leaf litterfall (dashed lines). Black symbols and lines represent PP plots (n = 4) and gray lines and symbols represent forest stands, including the mean of the four PP plots (n = 3). An inverse relationships among PP plots were not significant for F^*_{soil} and TBCF (r^2 = 0.65 and 0.75, P = 0.19 and 0.13, respectively). (b) Interannual variability in soil CO_2 flux (F_{soil}; expressed as yearly F_{soil} minus the interannual mean of F_{soil}) as a function of growing season water availability index (WAI, precipitation minus pan evaporation).

F_{soil} (Eq. (2), Fig. 2a and b). The sensitivity of F^*_{soil} to T_{10} was similar among PP plots (Fig. 2a). Differences in Q_{10} among PP plots were offset by the inverse correlation between Q_{10} and R_{b10}. But, among stands, PP showed the greatest sensitivity of F^*_{soil} to T_{10}, followed by HW, then OP (Fig. 2b and Table 2). Although support for a temporally constant Q_{10} can be found from comparisons of labile and recalcitrant soil carbon pools (Fang et al., 2005) to comparison among ecosystems over the globe (Mahecha et al., 2010), other studies showed a linear increase of root respiration with T_{soil} (i.e. decreasing Q_{10} with increasing T_{soil} over the growing season; Drake et al., 2008), and declining annual Q_{10} values after canopy closure (Bernhardt et al., 2006). The observed Q_{10} values were near the global means for broadleaf deciduous and evergreen needle forests and, as has been found in a global synthesis (Wang et al., 2010), Q_{10} increased with litterfall (Fig. 6a) but was unrelated to deciduousness. Supporting our second hypothesis (H2), Q_{10} and the overall temperature sensitivity of F^*_{soil} increased with leaf litterfall across our forest stands. However, in contrast to the expected decrease in the temperature sensitivity with increased leaf production (H3.a), the variation of these parameters among PP plots was small and unexplainable by either leaf litterfall or LAI. Instead, consistent with (H3.b), higher LAI tended to correspond with lower T_{10} (Fig. 7b), such that plot-level T_{10} explained as much of the variability in F^*_{soil} as LAI (Fig. 7c and d).

All stands showed reductions in F_{soil} from F^*_{soil} (i.e. lower f(REW)) under dry conditions. In contrast to the temperature sensitivity of F^*_{soil}, the sensitivity of the flux to soil water availability was similar among stands despite differences in soil texture (sandy-loam soil of OP versus clay-loam soil of the other two stands) and in growth habits (deciduous versus evergreen). Although parameters of the soil moisture sensitivity function differed among PP plots, their variation was unrelated to the LAI or litterfall. Drought-induced reduction of GPP will limit carbohydrate supply belowground and may also induce variation in the temperature sensitivity of F^*_{soil} inter-annually or during and after a drought cycle. While seasonal variation of basal rate of respiration has been shown vary with C uptake (Sampson et al., 2007), in our study, inter-annual variation of R_{b10} was unrelated to variation in water availability, the resource with the greatest influence on inter-annual variation of net primary production (McCarthy et al., 2010). At shorter timescales, based on estimated transport times (Mencuccini and Hölttä, 2010; Stoy et al., 2007), the recovery of F_{soil} from drought would lag precipitation 2–5 days. However, given the complexity of covarying factors contributing to the time lag between photosynthesis and F_{soil} (Kuzyakov and Gavrichkova, 2010) and the limitations to our experimental design, we could not directly link photosynthesis to F_{soil} at these time scales.

Summarizing the results related to H2, we demonstrated that the parameters capturing F^*_{soil}-sensitivity to T_{soil} differed among stands in relation to leaf litterfall, and were insensitive to inter-annual variation in soil moisture or stand characteristics. Furthermore, the stands shared a similar f(REW). In contrast, F^*_{soil} of PP plots showed similar overall sensitivity to T_{soil} but, for unknown reason, differences in f(REW) parameters. These responses interact with stand and plot T_{10} and REW to produce the observed annual F_{soil}, and its inter-annual and spatial variation.

Annual and growing season mean T_{10} was nearly invariable in all stands (Table 3), and in support of our first hypothesis (H1), REW was the dominant source of inter-annual variability of F_{soil}. Limitations of REW are expected to reduce photosynthesis through stomatal regulation (Oren and Pataki, 2001; Schäfer et al., 2002), which will, in turn, likely lead to reductions in both belowground production and respiration. For example, annual fine root respiration at PP was estimated at 645 g C m^{-2} (Drake et al., 2008), a sizable portion of F_{soil}, so an observed water availability-induced variation of fine root production at PP (Pritchard et al., 2008) could cause large variation of F_{soil}. Indeed, differences in the drought-related reductions in F_{soil} were driven by the frequency of low soil moisture days (inset in Fig. 2d), and resulted in that the inter-annual variation of F_{soil} roughly corresponded to the inter-annual variation in *annual* f(REW) (Fig. 3c). Thus, greater drought-induced reductions of F_{soil} at PP are not due to greater sensitivity to soil moisture than other stands, but rather, lower REW at PP due to an earlier start to the growing season than the deciduous HW stand (evident from the initiation of the decline in REW in Fig. 1b and the increase in evapotranspiration; see Stoy et al., 2006, Fig. 4c) and a shallower rooting zone than OP. For these reasons, in addition to greater canopy and litter interception of precipitation, annual f(REW) was lower at a given growing season WAI at PP than in the other stands (Fig. 4b). All stands, however, subscribed to a single relationship when growing season REW was used (Fig. 4a) thus providing a common soil moisture-based function to account for the inter-annual variation of F_{soil}. As result, the inter-annual variation of F_{soil}, expressed as a difference from the inter-annual mean of each stand, was largely explained by the corresponding variation of WAI (Fig. 5b). We attribute the lower intercept of annual f(REW) at

PP to higher rainfall interception loses at PP (compare Schäfer et al., 2002 with Oishi et al., 2010) and higher overall evapotranspiration (Stoy et al., 2006).

Inter-annual mean F_{soil} varied spatially among plots and stands and these differences were of similar magnitude to the inter-annual temporal variations at each plot and stand (Fig. 3a and b). We showed that temporal variation in F_{soil} at an annual scale was largely explained by REW, and now focus on an explanation for the spatial variation. Among stands, the inter-annual mean F^*_{soil} increased with leaf litterfall (Fig. 5a), as has been reported in earlier studies (Chen et al., 2010; Davidson et al., 2002; Palmroth et al., 2006). A rough estimate of TBCF (assuming steady-state litter and soil C pools) across our three stands shows that even after subtracting the effect of leaf litterfall, which accounts for ~20% of F_{soil}, the flux still increases with leaf litterfall (Fig. 5a). Furthermore, the relationship tended to reverse among plots of PP, showing decreasing F_{soil} (as well as TBCF) with increasing litterfall. These results demonstrate that litterfall is not a unique indicator of stand and site factors controlling TBCF and F_{soil}. Among the reasons, for example, leaf litterfall was well correlated with LAI among PP plots (Fig. 7a) but not among stands. Furthermore, annual litterfall is not sensitive to leaf phenology, yet earlier budbreak of deciduous trees can reduce springtime T_{soil} and REW, meaning it is the inter-annual dynamics of LAI rather than a representative value of LAI that affect annual F_{soil} (Phillips et al., 2010). Indeed, HW, the site with the highest peak growing season LAI and lowest winter LAI, had the highest growing season T_{10} (Fig. 1 and Table 3), which was likely influenced by a more heterogeneous stand structure and thinner growing season litter layer at HW than PP. This highlights the importance of accounting for LAI dynamics, horizontal heterogeneity in canopy cover, litter quality, and probably soil thermal properties when attempting to explain the variation of F_{soil} among stands of *different* structural attributes.

Summarizing results relevant to the hypothesized patterns across stands, the increased T_{soil}-sensitivity of F_{soil} with litterfall (Fig. 6) suggest that differences in productivity and TBCF among forests, rather than the relatively small differences in climatic forcing (e.g. higher T_{10} in HW and lower REW in PP), determined among-stand variation of F_{soil}, thus supporting H2.

Within PP, LAI varied among plots, reflecting nitrogen availability (McCarthy et al., 2006). Higher LAI reduced T_{10} (Fig. 7b) by increasing radiation attenuation and, given the similar temperature response (Fig. 1a and Table 4), reduced F^*_{soil} (Fig. 7c). However, because LAI integrates spatial variation of radiation reaching the forest floor, soil nutrient status, primary productivity, and carbon allocation among stands of similar attributes, LAI explains the spatial variation of F_{soil} better than leaf litterfall alone (Fig. 7d). The analyses presented here show LAI and T_{10} to explain the variation of F^*_{soil} equally well (Fig. 7c and d), leaving unanswered the question, does lower F^*_{soil} with higher LAI reflect a reduction of TBCF with increased plot fertility, or simply reflect lower respiration due to lower soil temperature? The minor range of LAI among the four PP plots used in this study makes it difficult to answer the question. However, Palmroth et al. (2006) observed among several temperate forests an inverse relationship between F_{soil} and LAI (normalized by proportion of year in growing season) ranging from approximately 1–5 $m^2\ m^{-2}$. Furthermore, a focused analysis of the four $CO_2 \times N$ treatments at Duke FACE, in which treatments induced a wider range of LAI, had a similar outcome (Oishi et al., in preparation); neither of the studies show a clear positive relationships between F^*_{soil} and soil temperature. Finally, elevated CO_2 induced 14% higher LAI (McCarthy et al., 2007). Thus, had lower T_{10} due to higher LAI reduced autotrophic and heterotrophic respiration rates, soil C would have increased in plots under elevated CO_2 relative to ambient plots—yet no such increase was detected (Lichter et al., 2008). Thus we suggest that the relationships of F^*_{soil}

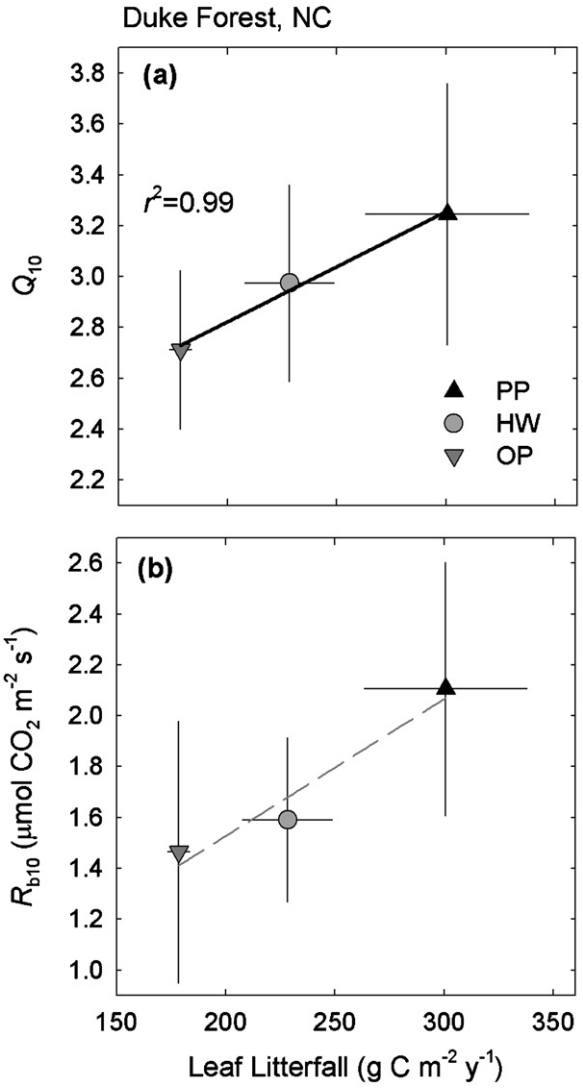

Fig. 6. Stand-level annual leaf litterfall and (a) Q_{10} and (b) basal respiration at 10 °C (R_{b10}; r^2 = 0.94, but P = 0.14). Error bars represent 1 SD.

with T_{10} are corollary to changes in LAI, reflecting decreased TBCF with increasing LAI in support of H3.a (Palmroth et al., 2006) rather than decreasing respiration with soil temperature in contrast to H3.b.

An inverse relationship between LAI and F_{soil} has been observed within other forest stands. In a European beech forest, plots with higher LAI had lower R_{b10} and thus, lower growing season F_{soil} (Ngao et al., 2012). The authors attributed this trend to greater soil water limitations in plots with higher LAI, caused by greater transpiration and precipitation interception. We found that mean growing season REW was lowest in PP where mean annual LAI was greatest relative to the other stands (Tables 1 and 3); however, among PP plots, REW was similar and among stands, no trend with LAI was observed. Thus, while differences in the soil moisture reduction functions (f(REW)) among PP plots contributed to interannual variability in F_{soil}, we demonstrate that spatial variability in F^*_{soil} resulted from a combination of differences in T_{10} and Q_{10}, both of which may reflect decreasing TBCF with increasing LAI (Fig. 7).

In a recent global synthesis, Bahn et al. (2010) combined site-specific estimates of base respiration and Q_{10} with mean annual T_{soil} to calculate F_{soil} at mean annual T_{soil} (Fig. 8a). As expected, annual F_{soil} was related to the rate of F_{soil} at mean annual T_{soil}, but

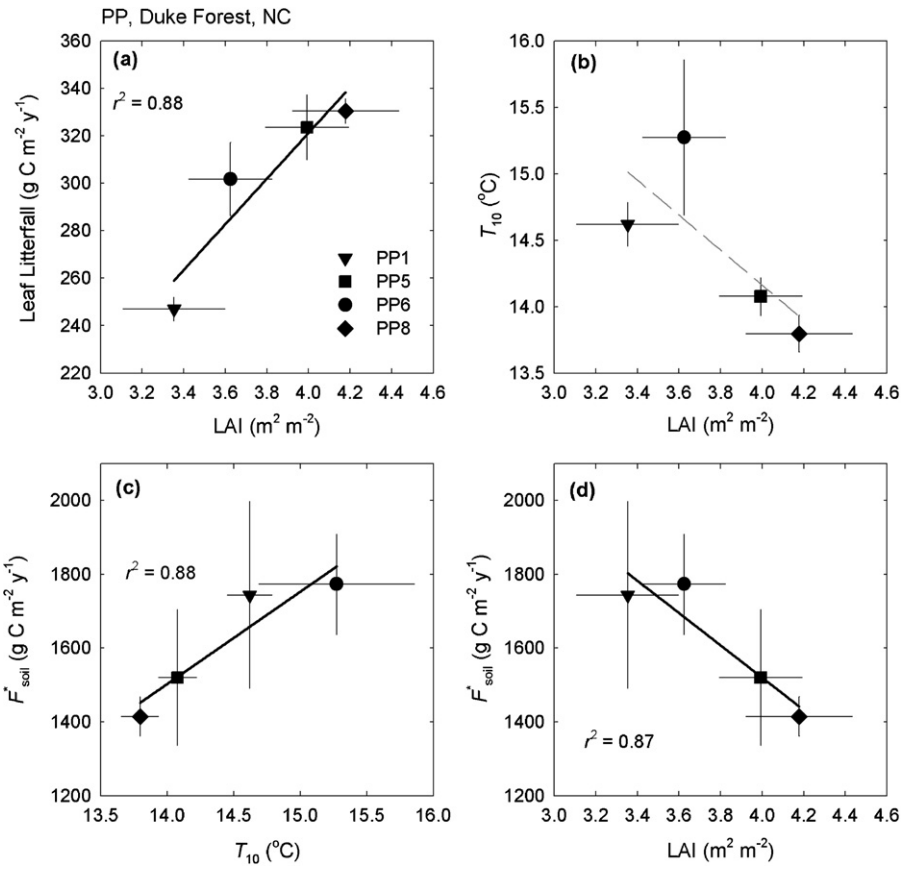

Fig. 7. Mean annual leaf area index (LAI) compared to (a) leaf litter and (b) mean annual soil temperature at 10 cm (T_{10}; $r^2 = 0.56$, but $P = 0.25$). Potential soil CO_2 flux under non-limiting soil moisture conditions (F^*_{soil}) as a function of (c) mean annual T_{10} and (d) mean annual LAI. Solid lines are significant at $P < 0.10$.

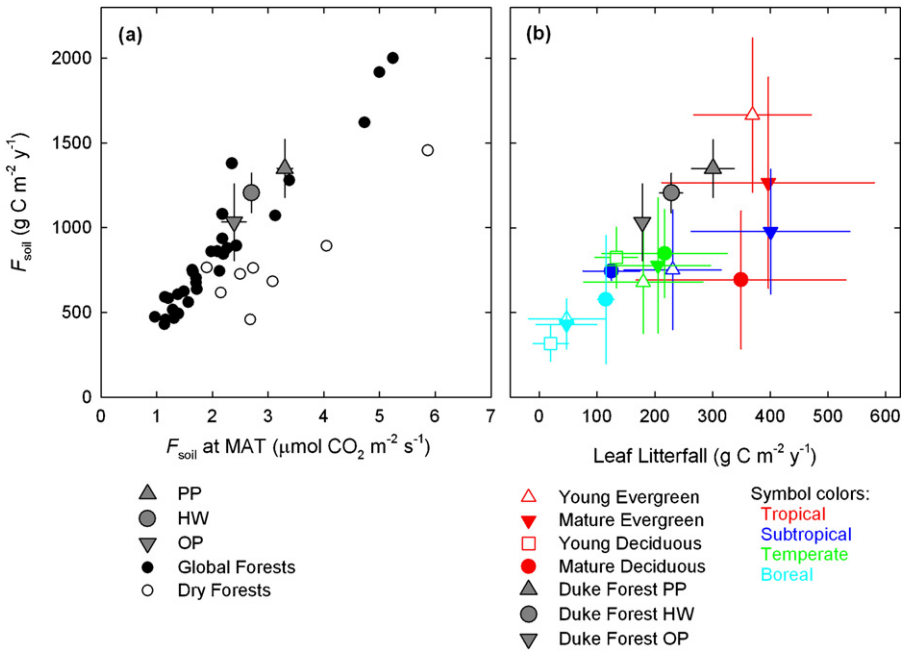

Fig. 8. Global trends in forest soil CO_2 flux (F_{soil}) as a function of (a) F_{soil} at mean annual soil temperature (MAT), separated by mesic and dry (Mediterranean, sub-humid, and semiarid; data from forests ecosystems from Bahn et al. (2010), averaged over years for a given site) and (b) annual leaf litter from the Global Soil Respiration Database (Bond-Lamberty and Thomson, 2010; version "20110524a", download date 1/29/2012, http://code.google.com/p/srdb; data from untreated stands, averaged over years for a given site), separated by biome, evergreen/deciduous, and age group (aggrading or mature). Error bars represent 1 SD.

neither Q_{10} nor annual F_{soil} were related to soil temperature. Using this approach, which explicitly considers T_{soil}, the rank of annual F_{soil} among our stands was preserved, and our estimates were close to those expected based on the global relationship, averaging 8% higher (+4% at PP and +10% at HW and OP, Fig. 8a).

We also compared our results to a global dataset presented by Bond-Lamberty and Thomson (2010). Our reanalysis shows that the relationship between F_{soil} and litterfall does not hold for stands within any subcategory of forests (e.g. young or mature, evergreen or deciduous), or among categories, with the exception of boreal forests (Fig. 8b). The overall relationship emerges mostly at the scale of biomes. Interestingly, our forests experienced near the upper range of the flux data, reflecting the relatively warm nature of the US southeast (~15 °C versus ~10 °C for many of the other temperate forests) or the inclusion of fine woody material as litterfall, which was excluded by some of these studies (Bond-Lamberty and Thomson, 2010). The relationship clearly does not imply that litterfall controls F_{soil}, because on average litterfall accounts for roughly a third of the flux; litterfall is but an indicator of stand and site factors controlling TBCF. Another such factor that covaries with overall productivity across biomes is T_{soil}. It decreases poleward with radiation, and among stands with similar characteristics, it decreases with increasing LAI.

Thus, among stands, increased photosynthesis associated with higher LAI or more supportive climate (i.e. higher temperatures and lower water stress), along with increased decomposable litter appears to lead to increases in F_{soil}. However, within a stand, higher LAI can be correlated to two potential mechanisms for reductions in F_{soil}: lower radiative load heating of the soil and reduced allocation of carbon to belowground uses. These results suggest that including some simple forest characteristics, such as stand composition and LAI, with regional measurements of temperature and water stress, will help to explain the variability in F_{soil} among plots within biomes.

Acknowledgments

This research was supported by the Office of Science (BER) of US Department of Energy through Terrestrial Carbon Processes (TCP) program (FACE, DE-FG02-95ER62083 and proposal 11-DE-SC-0006700 – grant ER65189), by the National Institute of Global Environmental Change (NIGEC) through the Southeast Regional Center at the University of Alabama, Tuscaloosa (DOE cooperative agreement DE-FC030-90ER61010), and by the SERC-NIGEC RCIAP Research Program. We thank Daniel McInnis for technical assistance with the ACES and field support.

Appendix A. Soil moisture measurements

Cross-correlation of cleaned data from the two different sensors types installed concurrently at PP8 showed significant linear relationships ($P < 0.001$) in all pairings, and CS-615s were not consistently higher or lower than ML2x probes at shallow or deep depths or averaged across depths. Mean r^2 among different sensors was 0.68 (SD = 0.11), slightly lower than correlation among ML2x probes ($r^2 = 0.77$, SD = 0.08, t-test $P = 0.001$) and not significantly lower than correlation among CS-615 probes ($r^2 = 0.75$, SD = 0.12, t-test $P = 0.20$). Periods where θ reached field capacity or the hygroscopic minimum were identified and the recorded values for each sensor were rescaled to match these values. Missing data, due to power outages in one of the plots or sensor failure, were gap-filled using the best linear regressions with other working sensors. The regressions were comprised of data on both sides of the gap, equal to the length of the gap in each direction.

Appendix B. Leaf litter replenishment under soil chambers

Although chambers do temporarily exclude leaf litter, we replenished litter with all biomass components in one of two ways. In PP8 up to 2005, HW, and OP, litter was collected in baskets, harvested weekly during peak litterfall and monthly to bi-monthly the rest of the year, weighed and redistributed at the chamber location to maintain a similar input per unit ground area. After the deployment of ACES in all FACE plots in 2005, the protocol was changed to redistribute litter that accumulated on the chamber top each time location was switched (twice weekly). The revised approach was designed to solve two issues, (1) it immediately replaced litter that had been excluded, preventing a lag in measurements and drying while the litter remained in the basket, and (2) it provided a more similar quantity and quality of litter that reflected the within-plot species distribution. We assessed the likely effect of the changed approach setting up a study in a 5×5 m plot adjacent to PP6 and compared litter collected in two baskets (0.5 m^2 each) with 8 "dummy" chambers during the peak of leaf fall, from mid-September through early December. The chamber-top litter approach collected approximately 15% more (SD = 12%) litter than the basket method, but the amount was not significantly different ($P > 0.05$) during 13 out of 17 collection periods. The revised approach has likely resulted in an addition of 50 g C m^{-2} y^{-1} in litter added to the chamber footprint, or less than 5% of previously reported annual F_{soil} from this site (1231–1330 g C m^{-2} y^{-1}; Palmroth et al., 2005).

Appendix C. Temperature response model performance

Data from profile measurements (Daly et al., 2009) revealed that the time of day T_{soil} reached its peak was similar at all depths and for all months ($P > 0.06$), and that using daily mean T_{soil} from either 5 or 10 cm depth produced similar estimates of annual F_{soil} ($P = 0.32$), justifying gap-filling daily F_{soil} using more consistently available T_{10}.

In order to compare the exponential model with other commonly used function, we fit location data for PP8 under non-limiting soil moisture conditions (REW > 0.33). A modified Arrhenius equation (Lloyd and Taylor, 1994) explained only ~1% more of the variation and did not lead to a significant difference in annual numbers (<1%; t-test $P = 0.87$). We also attempted to test for different temperature sensitivities between winter (where contribution of recently assimilated carbon is nearly or entirely eliminated) and summer. This approach did not yield useful results because extrapolating exponential function derived based on highly scattered data outside of the data range led to many unreasonable predictions at higher temperatures. Furthermore, large variability of F_{soil} during the growing season (even after filtering out low REW conditions) often did not produce significant fits ($P > 0.05$, 32% of growing season fits).

Appendix D. Supplementary data

Supplementary data associated with this article can be found, in the online version, at http://dx.doi.org/10.1016/j.agrformet.2012.12.007.

References

Bahn, M., Reichstein, M., Davidson, E.A., Grünzweig, J., Jung, M., Carbone, M.S., Epron, D., Misson, L., Nouvellon, Y., Roupsard, O., Savage, K., Trumbore, S.E., Gimeno, C., Curiel Yuste, J., Tang, J., Vargas, R., Janssens, I.A., 2010. Soil respiration at mean annual temperature predicts annual total across vegetation types and biomes. Biogeosciences 7 (7), 2147–2157.

Bernhardt, E.S., Barber, J.J., Pippen, J.S., Taneva, L., Andrews, J.A., Schlesinger, W.H., 2006. Long-term effects of free air CO_2 enrichment (FACE) on soil respiration. Biogeochemistry 77 (1), 91–116.
Bond-Lamberty, B., Thomson, A., 2010. A global database of soil respiration data. Biogeosciences 7 (6), 1915–1926.
Butnor, J.R., Johnsen, K.H., Oren, R., Katul, G.G., 2003. Reduction of forest floor respiration by fertilization on both carbon dioxide-enriched and reference 17-year-old loblolly pine stands. Global Change Biol. 9, 849–861.
Chen, G.-S., Yang, Y.-S., Guo, J.-F., Xie, J.-S., Yang, Z.-J., 2010. Relationships between carbon allocation and partitioning of soil respiration across world mature forests. Plant Ecol. 212 (2), 195–206.
Curiel Yuste, J., Nagy, M., Janssens, I.A., Carrara, A., Ceulemans, R., 2005. Soil respiration in a mixed temperate forest and its contribution to total ecosystem respiration. Tree Physiol. 25, 609–619.
Daly, E., Palmroth, S., Stoy, P., Siqueira, M., Oishi, A.C., Juang, J.-Y., Oren, R., Porporato, A., Katul, G.G., 2009. The effects of elevated atmospheric CO_2 and nitrogen amendments on subsurface CO_2 production and concentration dynamics in a maturing pine forest. Biogeochemistry 94 (3), 271–287.
Davidson, E.A., Janssens, I.A., 2006. Temperature sensitivity of soil carbon decomposition and feedbacks to climate change. Nature 440 (7081), 165–173.
Davidson, E.A., Janssens, I.A., Luo, Y., 2006. On the variability of respiration in terrestrial ecosystems: moving beyond Q_{10}. Global Change Biol. 12, 154–164.
Davidson, E.A., Savage, K., Bolstad, P.V., Clark, D.A., Curtis, P.S., Ellsworth, D.S., Hanson, P.J., Law, B.E., Luo, Y., Pregitzer, K.S., Randolph, J.C., Zak, D., 2002. Belowground carbon allocation in forests estimated from litterfall and IRGA-based soil respiration measurements. Agric. For. Meteorol. 113, 39–51.
DeLucia, E.H., Drake, J.E., Thomas, R.B., Gonzalez-Meler, M., 2007. Forest carbon use efficiency: is respiration a constant fraction of gross primary production? Global Change Biol. 13, 1157–1167.
Drake, J.E., Oishi, A.C., Giasson, M.-A., Oren, R., Johnsen, K.H., Finzi, A.C., 2012. Trenching reduces soil heterotrophic activity in a loblolly pine (*Pinus taeda*) forest exposed to elevated atmospheric [CO_2] and N fertilization. Agric. For. Meteorol. 165, 43–52, http://dx.doi.org/10.1016/j.agrformet.2012.05.017.
Drake, J.E., Stoy, P.C., Jackson, R.B., DeLucia, E.H., 2008. Fine-root respiration in a loblolly pine (*Pinus taeda* L.) forest exposed to elevated CO_2 and N fertilization. Plant Cell Environ. 31 (11), 1663–1672.
Fang, C., Moncrieff, J.B., 2001. The dependence of soil CO_2 efflux on temperature. Soil Biol. Biochem. 33, 155–165.
Fang, C., Smith, P., Moncrieff, J.B., Smith, J.U., 2005. Similar response of labile and resistant soil organic matter pools to changes in temperature. Nature 433, 57–59.
Fenn, K.M., Malhi, Y., Morecroft, M.D., 2010. Soil CO_2 efflux in a temperate deciduous forest: environmental drivers and component contributions. Soil Biol. Biochem. 42 (10), 1685–1693.
Gaumont-Guay, D., Black, T.A., Griffis, T.J., Barr, A.G., Jassal, R.S., Nesic, Z., 2006. Interpreting the dependence of soil respiration on soil temperature and water content in a boreal aspen stand. Agric. For. Meteorol. 140 (1–4), 220–235.
Giardina, C.P., Ryan, M.G., 2002. Total belowground carbon allocation in a fast-growing eucalyptus plantation estimated using a carbon balance approach. Ecosystems 5, 487–499.
Granier, A., 1987. Sap flow measurements in Douglas fir tree trunks by means of a new thermal method. Ann. Sci. Forest. 44, 1–14.
Högberg, P., Högberg, M.N., Gottlicher, S.G., Betson, N.R., Keel, S.G., Metcalfe, D.B., Campbell, C., Schindlbacher, A., Hurry, V., Lundmark, T., Linder, S., Nasholm, T., 2008. High temporal resolution tracing of photosynthate carbon from the tree canopy to forest soil microorganisms. New Phytol. 177 (1), 220–228.
Irvine, J., Law, B.E., Martin, J.G., Vickers, D., 2008. Interannual variation in soil CO_2 efflux and the response of root respiration to climate and canopy gas exchange in mature ponderosa pine. Global Change Biol. 14 (12), 2848–2859.
Janssens, I.A., Lankreijer, H., Matteucci, G., Kowalski, A.S., Buchmann, N., Epron, D., Pilegaard, K., Kutsch, W.L., Longdoz, B., Grunwald, T., Montagnani, L., Dore, S., Rebmann, C., Moors, E.J., Grelle, A., Rannik, U., Morgenstern, K., Oltchev, S., Clement, R., Gudmundsson, J., Minerbi, S., Berbigier, P., Ibrom, A., Moncrieff, J.B., Aubinet, M., Bernhofer, C., Jensen, O.P., Vesala, T., Granier, A., Schulze, E.D., Lindroth, A., Dolman, A.J., Ceulemans, R., Valentini, R., 2001. Productivity overshadows temperature in determining soil and ecosystem respiration across European forests. Global Change Biol. 7, 269–278.
Johnsen, K., Maier, C., Sanchez, F., Anderson, P., Butnor, J., Waring, R., Linder, S., 2007. Physiological girdling of pine trees via phloem chilling: proof of concept. Plant Cell Environ. 30 (1), 128–134.
Kuzyakov, Y., Gavrichkova, O., 2010. Time lag between photosynthesis and carbon dioxide efflux from soil: a review of mechanisms and controls. Global Change Biol. 16, 3386–3406.
Lichter, J., Billings, S.A., Ziegler, S.E., Gaindh, D., Ryals, R., Finzi, A.C., Jackson, R.B., Stemmler, E.A., Schlesinger, W.H., 2008. Soil carbon sequestration in a pine forest after 9 years of atmospheric CO_2 enrichment. Global Change Biol. 14 (12), 2910–2922.
Litton, C.M., Raich, J.W., Ryan, M.G., 2007. Carbon allocation in forest ecosystems. Global Change Biol. 13 (10), 2089–2109.
Lloyd, J., Taylor, J.A., 1994. On the temperature dependence of soil respiration. Funct. Ecol. 8, 315–323.
Luan, J., Liu, S., Zhu, X., Wang, J., Liu, K., 2012. Roles of biotic and abiotic variables in determining spatial variation of soil respiration in secondary oak and planted pine forests. Soil Biol. Biochem. 44, 143–150.
Mahecha, M.D., Reichstein, M., Carvalhais, N., Lasslop, G., Lange, H., Seneviratne, S.I., Vargas, R., Ammann, C., Arain, M.A., Cescatti, A., Janssens, I.A., Migliavacca, M., Montagnani, L., Richardson, A.D., 2010. Global convergence in the temperature sensitivity of respiration at ecosystem level. Science 329 (5993), 838–840.
Maier, C.A., Albaugh, T.J., Allen, H.L., Dougherty, P.M., 2004. Respiratory carbon use and carbon storage in mid-rotation loblolly pine (*Pinus taeda* L.) plantations: the effect of site resources on the stand carbon balance. Global Change Biol. 10, 1335–1350.
Maier, M., Schack-Kirchner, H., Hildebrand, E.E., Schindler, D., 2011. Soil CO_2 efflux vs. soil respiration: implications for flux models. Agric. For. Meteorol. 151 (12), 1723–1730.
Martin, J.G., Bolstad, P.V., 2009. Variation of soil respiration at three spatial scales: components within measurements, intra-site variation and patterns on the landscape. Soil Biol. Biochem. 41 (3), 530–543.
McCarthy, H.R., Oren, R., Finzi, A.C., Johnsen, K.H., 2006. Canopy leaf area constrains [CO_2]-induced enhancement of productivity and partitioning among aboveground carbon pools. Proc. Natl. Acad. Sci. U.S.A. 103, 19356–19361.
McCarthy, H.R., Oren, R., Johnsen, K.H., Gallet-Budynek, A., Pritchard, S.G., Cook, C.W., Ladeau, S.L., Jackson, R.B., Finzi, A.C., 2010. Re-assessment of plant carbon dynamics at the Duke free-air CO_2 enrichment site: interactions of atmospheric [CO_2] with nitrogen and water availability over stand development. New Phytol. 185 (2), 514–528.
McCarthy, H.R., Oren, R., Finzi, A.C., Ellsworth, D.S., Kim, H.-S., Johnsen, K.H., Millar, B., 2007. Temporal dynamics and spatial variability in the enhancement of canopy leaf area under elevated atmospheric CO_2. Global Change Biol. 13 (12), 2479–2497.
Mencuccini, M., Hölttä, T., 2010. The significance of phloem transport for the speed with which canopy photosynthesis and belowground respiration are linked. New Phytol. 185 (1), 189–203.
Moyano, F.E., Kutsch, W.L., Rebmann, C., 2008. Soil respiration fluxes in relation to photosynthetic activity in broad-leaf and needle-leaf forest stands. Agric. For. Meteorol. 148 (1), 135–143.
Nadelhoffer, K.J., Raich, J.W., 1992. Fine root production estimates and belowground carbon allocation in forest ecosystems. Ecology 73, 1139–1147.
Ngao, J., Epron, D., Delpierre, N., Breda, N., Granier, A., Longdoz, B., 2012. Spatial variability of soil CO_2 efflux linked to soil parameters and ecosystem characteristics in a temperate beech forest. Agric. For. Meteorol. 154–155, 136–146.
Oishi, A.C., Oren, R., Stoy, P.C., 2008. Estimating components of forest evapotranspiration: a footprint approach for scaling sap flux measurements. Agric. For. Meteorol. 148, 1719–1732.
Oishi, A.C., Oren, R., Novick, K.A., Palmroth, S., Katul, G.G., 2010. Interannual Invariability of Forest Evapotranspiration and Its Consequence to Water Flow Downstream. Ecosystems 13 (3), 421–436.
Oishi, A.C., Palmroth, S., Johnsen, K.H., McCarthy, H.R. and Oren, R., in preparation. Effects of atmospheric [CO_2], nitrogen availability and soil moisture on the spatial and temporal variation of forest soil CO_2 flux. Global Change Biol.
Oren, R., Pataki, D.E., 2001. Transpiration in response to variation in microclimate and soil moisture in southeastern deciduous forests. Oecologia 127, 549–559.
Oren, R., Phillips, N., Katul, G.G., Ewers, B.E., Pataki, D.E., 1998. Scaling xylem sap flux and soil water balance and calculating variance: a method for partitioning water flux in forests. Ann. Sci. For. 55, 191–216.
Palmroth, S., Maier, C.A., McCarthy, H.R., Oishi, A.C., Kim, H.-S., Johnsen, K.H., Katul, G.G., Oren, R., 2005. Contrasting responses to drought of forest floor CO_2 efflux in a Loblolly pine plantation and a nearby Oak-Hickory forest. Global Change Biol. 11, 421–434.
Palmroth, S., Oren, R., McCarthy, H.R., Johnsen, K.H., Finzi, A.C., Butnor, J.R., Ryan, M.G., Schlesinger, W.H., 2006. Aboveground sink strength in forests controls the allocation of carbon below ground and its [CO_2]-induced enhancement. Proc. Natl. Acad. Sci. U.S.A. 103 (51), 19362–19367.
Phillips, C.L., Nickerson, N., Risk, D., Bond, B.J., 2011. Interpreting diel hysteresis between soil respiration and temperature. Global Change Biol. 17 (1), 515–527.
Phillips, S.C., Varner, R.K., Frolking, S., Munger, J.W., Bubier, J.L., Wofsy, S.C., Crill, P.M., 2010. Interannual, seasonal, and diel variation in soil respiration relative to ecosystem respiration at a wetland to upland slope at Harvard Forest. J. Geophys. Res. 115 (G2).
Pritchard, S.G., Strand, A.E., McCormack, M.L., Davis, M.A., Finzi, A.C., Jackson, R.B., Matamala, R., Rogers, H.H., Oren, R., 2008. Fine root dynamics in a loblolly pine forest are influenced by free-air-CO_2-enrichment: a six-year-minirhizotron study. Global Change Biol. 14 (3), 588–602.
Raich, J.W., Schlesinger, W.H., 1992. The global carbon-dioxide flux in soil respiration and its relationship to vegetation and climate. Tellus Ser. B: Chem. Phys. Meteorol. 44 (2), 81–99.
Reichstein, M., Rey, A., Freibauer, A., Tenhunen, J., Valentini, R., Banza, J., Casals, P., Cheng, Y., Grunzweig, J., Irvine, J., Joffre, R., Law, B., Loustau, D., Miglietta, F., Oechel, W., Ourcival, J., Pereira, J., Peressotti, A., Ponti, F., Qi, Y., Rambal, S., Rayment, M., Romanya, J., Rossi, F., Tedeschi, V., Tirone, G., Xu, M., Yakir, D., 2003. Modeling temporal and large-scale spatial variability of soil respiration from soil water availability, temperature and vegetation productivity indices. Global Biogeochem. Cycles 17, 1104.
Risk, D., Kellman, L., Beltrami, H., 2002. Carbon dioxide in soil profiles: production and temperature dependence. Geophys. Res. Lett. 29 (6).
Riveros-Iregui, D.A., Emanuel, R.E., Muth, D.J., McGlynn, B.L., Epstein, H.E., Welsch, D.L., Pacific, V.J., Wraith, J.M., 2007. Diurnal hysteresis between soil CO_2 and soil temperature is controlled by soil water content. Geophys. Res. Lett. 34 (17).
Ryan, M.G., Law, B.E., 2005. Interpreting, measuring, and modeling soil respiration. Biogeochemistry 2005, 3–27.

Sampson, D.A., Janssens, I.A., Curiel Yuste, J., Ceulemans, R., 2007. Basal rates of soil respiration are correlated with photosynthesis in a mixed temperate forest. Global Change Biol. 13 (9), 2008–2017.

Savage, K., Davidson, E.A., Richardson, A.D., Hollinger, D.Y., 2009. Three scales of temporal resolution from automated soil respiration measurements. Agric. For. Meteorol. 149 (11), 2012–2021.

Schäfer, K.V.R., Oren, R., Lai, C.-T., Katul, G.G., 2002. Hydrologic balance in an intact temperate forest ecosystem under ambient and elevated atmospheric CO_2 concentration. Global Change Biol. 8, 895–911.

Schimel, D.S., House, J.I., Hibbard, K.A., Bousquet, P., Ciais, P., Peylin, P., Braswell, B.H., Apps, M.J., Baker, D., Bondeau, A., Canadell, J., Churkina, G., Cramer, W., Denning, A.S., Field, C.B., Friedlingstein, P., Goodale, C., Heimann, M., Houghton, R.A., Melillo, J.M., Moore III, B., Murdiyarso, D., Noble, I., Pacala, S.W., Prentice, I.C., Raupach, M.R., Rayner, P.J., Scholes, R.J., Steffen, W.L., Wirth, C., 2001. Recent patterns and mechanisms of carbon exchange by terrestrial ecosystems. Nature 414, 169–172.

Søe, A.R.B., Buchmann, N., 2005. Spatial and temporal variations in soil respiration in relation to stand structure and soil parameters in an unmanaged beech forest. Tree Physiol. 25, 1427–1436.

Stoy, P.C., Katul, G.G., Siqueira, M.B.S., Juang, J.-Y., Novick, K.A., McCarthy, H.R., Oishi, A.C., Uebelherr, J.M., Kim, H.-S., Oren, R., 2006. Separating the effects of climate and vegetation on evapotranspiration along a successional chronosequence in the southeastern US. Global Change Biol. 12 (11), 2115–2135.

Stoy, P.C., Palmroth, S., Oishi, A.C., Siqueira, M.B., Juang, J.Y., Novick, K.A., Ward, E.J., Katul, G.G., Oren, R., 2007. Are ecosystem carbon inputs and outputs coupled at short time scales? A case study from adjacent pine and hardwood forests using impulse-response analysis. Plant Cell Environ. 30 (6), 700–710.

Subke, J.A., Bahn, M., 2010. On the 'temperature sensitivity' of soil respiration: Can we use the immeasurable to predict the unknown? Soil Biol. Biochem. 42 (9), 1653–1656.

Suwa, M., Katul, G.G., Oren, R., Andrews, J., Pippen, J., Mace, A., Schlesinger, W.H., 2004. Impact of elevated atmospheric CO_2 on forest floor respiration in a temperate pine forest. Global Biogeochem. Cycles 18 (2).

Taneva, L., Gonzalez-Meler, M.A., 2011. Distinct patterns in the diurnal and seasonal variability in four components of soil respiration in a temperate forest under free-air CO_2 enrichment. Biogeosciences 8 (10), 3077–3092.

Trumbore, S.E., 2000. Age of soil organic matter and soil respiration: radiocarbon constraints on belowground C dynamics. Ecol. Appl. 10 (2), 399–411.

United States Department of Agriculture, S.C.S., 1960. Soil Survey of Alamance County, North Carolina.

United States Department of Agriculture, S.C.S., 1977. Soil Survey of Orange County, North Carolina.

Wang, W., Chen, W., Wang, S., 2010. Forest soil respiration and its heterotrophic and autotrophic components: global patterns and responses to temperature and precipitation. Soil Biol. Biochem. 42, 1236–1244.